Design methodology for the mechanical reliability of optical fiber

G. S. Glaesemann
S. T. Gulati
Corning Incorporated
Sullivan Park
Corning, New York 14831

Abstract. An engineering methodology for the mechanical reliability of optical fiber is developed within a fracture-mechanics framework. The model expresses allowable in-service and installation stresses as a fraction of fiber strength in a fatigue environment for a range of n values and fiber types. Failure probability is incorporated into the model by the measurement of the fiber-strength distribution appropriate to the application. For long-length applications, strength distributions of hundreds to thousands of kilometers of fiber are needed. A 400-km strength distribution captures the beginnings of the truncated portion of the distribution.

CONTENTS

1. INTRODUCTION

It is well known that glass optical fibers exhibit delayed failure when stressed sufficiently in a moist environment. Small flaws on the fiber surface grow subcritically under these conditions to dimensions critical for failure. This phenomenon of subcritical crack growth is commonly referred to as fatigue, and has been described on a molecular scale by Michalske and Frieman[1] as "a specific chemical reaction between strained bonds in vitreous silica and water, which can be used to explain environmental enhanced crack growth."

For reliability purposes it is desirable that subcritical crack growth and the resulting strength degradation be stopped or kept to an acceptable minimum. One obvious method of stopping subcritical crack growth is to maintain a moisture-free fiber surface, which is the purpose behind the hermetic-coated fiber technology. In the case where the glass surface is exposed to moisture, we could keep the applied stress to a level below which no subcritical crack growth occurs over the lifetime of the fiber. The latter case involves the concept of a threshold for fatigue. The significance of a fatigue threshold is that fiber loaded below the threshold stress has no probability of failure and no strength degradation over the in-service lifetime. Such behavior has been observed in soda-lime glass but not in pure silica glass. However, we can approximate a threshold by simply choosing a stress value sufficiently low (or safe) that, for engineering purposes, the fiber is considered to be failure-free for life.

This paper presents a "safe" stress model for slow crack growth in glass optical fiber by employing an upper limit for slow crack growth that is considered safe from a reliability point of view. Classical fracture mechanics and conventional crack-kinetics theory[2] are used as a framework in developing the model. The model proves useful in developing the design methodology for long-term reliability of stressed optical fiber. Particular attention is paid to incorporating the strength distribution of long fibers in the design methodology.

2. CLASSICAL APPROACH TO RELIABILITY PREDICTIONS

The most common approach for making failure predictions is to employ the following static fatigue equation derived from the power law crack velocity relation:

$$t_f = BS_i^{n-2}\sigma_a^{-n},$$

where t_f is the time to failure under an applied stress σ_a, S_i is the inert of initial strength, and B and n are crack-growth parameters. The crack-growth resistance parameter n is obtained from the slope of static dynamic fatigue curves. Inert strength measurements are necessary to calculate the parameter B. However, such measurements are extremely difficult for most fiber lengths except those performed in parallel plate bending.[4] Furthermore, since inert tensile strength values used in Eq. (1) typically are obtained

using short gauge length specimens, their validity for long-length applications is questionable. In other words, it is difficult to use Eq. (1) in the context of long-length applications involving kilometers of fiber.

Our objective here is to develop a framework for reliability predictions that is practical from both engineering and experimental points of view. Thus, instead of the inert strength measurement and its length limitations, we incorporate the long-length strength distribution measured under fatigue conditions. A long-length strength distribution provides an engineering basis for a design methodology for low failure probability predictions and the experimental credibility to place it on a firm foundation.

3. THEORETICAL CONSIDERATIONS FOR A SAFE STRESS DESIGN

Nearly 12 years ago, Helfinstine of Corning loaded one-hundred, 2-m-long, lacquer-coated silica-clad fibers to a static stress of 30% of the 100-kpsi (690-MPa) proof stress in liquid water. To date, no fatigue failures have been reported. The lack of fiber failures strongly suggests that either no crack growth has occurred over the past decade of that crack velocities are extremely low. In addition to Helfinstine's static fatigue study, Gulati[2] published theoretical work that predicted no strength degradation for dynamic loading of fiber to more than 90% of its fast-fracture strength. He verified his predictions experimentally by conducting tensile tests on 1-m-long silica-clad fibers. This previous work gives sufficient impetus for pursuing the concept of safe stress for the static loading of optical fiber for decades.

3.1 Crack growth kinetics

It is well understood that flaws in glass subjected to tensile stress in the presence of moisture grow subcritically prior to failure.[5] Much research has been invested in this phenomenon, with the key finding that crack growth prior to failure can be separated into three distinct regions, as shown in Fig. 1. The stress intensity factor, K_I, in Fig. 1 relates the crack depth a to the applied stress σ through $K_I = Y\sigma\sqrt{a}$, where Y is a shape factor determined by crack geometry and loading conditions.[6] Region I is the region of stable (subcritical) crack growth where crack velocity V increases steadily with increasing K_I. In region II the crack has attained sufficient velocity to "out run" water transport to the crack tip. Region III is the region of unstable crack growth approaching the terminal crack velocity ($\approx$1500 m/s). It is important to note that in view of extremely low crack velocities, the crack spends the majority of its life in region I. Therefore, region I historically has received the greatest attention in lifetime modeling.
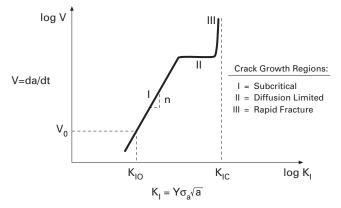

Fig. 1 Crack velocity versus stress intensity factor.

Many models have been proposed to describe the relationship between crack velocity and stress-intensity factor in region I.[7] The model that has received widest acceptance, due to its mathematical simplicity and empirical representation of fatigue data, is the power law[3,8]

$$V = AK_I^n$$

where A and n are crack-growth parameters. Equation (2) can be rewritten as

$$da/dt = A(Y\sigma\sqrt{a})^n$$

This equation represents the change in crack length with time due to applied stress in a corrosive environment.

3.2 Safe condition

We *define* a "safe" condition of upper bound for allowable subcritical crack growth as crack velocity $V = V_0$ sufficiently small that its contribution to crack growth would be considered insignificant over the fiber's lifetime. This "safe" velocity has an associated stress-intensity factor $K_{I0} = Y\sigma_0\sqrt{a_0}$, as shown in Fig. 1. Thus, from Eq. (3) $V_0 = A(Y\sigma_0\sqrt{a_0})^n$, represents the velocity of an initial crack of length a_0 growing under a static stress σ_0, which we define as the safe stress. Gulati[2] normalized Eq. (3) with $V_0 = A(Y\sigma_0\sqrt{a_0})^n$ by simply substituting $V_0(\sigma_0\sqrt{a_0})^{-n}$ for AY^n in Eq. (3), resulting in a nondimensional form of the power law equation.

$$\frac{V}{V_0} = \left(\frac{\sigma}{\sigma_0}\right)^n \left(\frac{a}{a_0}\right)^{n/2}$$

or

$$V = \frac{da}{dt} = V_0\left(\frac{\sigma}{\sigma_0}\right)^n \left(\frac{a}{a_0}\right)^{n/2}$$

Equation (5) can be rearranged and integrated with respect to time from time $t = 0$ to t and crack length $a = a_0$ to a, for any stress history:

$$\int_{a_0}^{a} \left(\frac{a}{a_0}\right)^{-n/2} da = V_0 \int_{0}^{t} \left(\frac{\sigma}{\sigma_0}\right)^n dt$$

For constant stress loading σ is a constant, $\sigma = \sigma_a$, and for dynamic loading σ is time dependent, $\sigma = \dot{\sigma}t$, with $\dot{\sigma}$ as the stressing rate. In this paper, only the static-stress condition will be considered. For a thorough treatment of dynamic stress condition, see Ref. 2.

Integration of Eq. (6) for a constant applied stress, $\sigma = \sigma_a$, gives the following relation for crack extension beyond its initial length a_0 as a function of time:

$$\frac{a}{a_0} = \left[1 - \left(\frac{n}{2} - 1\right)\frac{V_0}{a_0}\left(\frac{\sigma_a}{\sigma_0}\right)^n t\right]^{-2/(n-2)} \quad, \ n>2 \ .$$

Equation (7) describes the time dependence of crack growth beyond the initial length a_0 under an applied stress $\sigma_a \geq \sigma_0$. Note that Eq. (7) can be expressed in terms of the more classical power law crack velocity parameters by substituting $V_0(\sigma_0 \sqrt{a_0})^{-n} = AY^n$.

To obtain the crack growth parameter V_0/a_0, we use the threshold or "safe" boundary condition. We seek a boundary condition that limits the crack growth to an acceptable safe limit without compromising fiber reliability. Gulati[2] chose the conservative condition of 1% growth in 40 yr, or $a/a_0 = 1.01$ for $t = 40$ yr (1.26×10^9 s) at $\sigma_a = \sigma_0$. In other words, when we apply a constant stress σ_a equal to the safe stress σ_0 for 40 yr, only 1% growth of the initial crack is acceptable. This is equivalent to allowing 0.5% degradation in fiber strength, which, for engineering purposes, is considered insignificant. Admittedly, 1% crack growth is not a condition derived from fundamental considerations, rather it is a safe condition from which a useful engineering model can be developed.

When we substitute the above boundary condition into Eq. (7), we determine V_0/a_0 to be approximately 7.5×10^{-12} s^{-1} for a wide range of n values. For the range of V_0/a_0 values in Table 1, the predicted σ_0 varies by less than 1% for given t, σ_a, and n. Thus, V_0/a_0 in the range $15<n<45$ can be considered a constant. For other values of n the dependence of V_0/a_0 on n can be readily calculated using Eq. (7). For example, for hermetic fiber with a typical n value of 200, V_0/a_0 is determined to be 5×10^{-12} s^{-1} for 40-yr life.

Having determined V_0/a_o, we now can plot crack growth a/a_0 versus time t for a given n value and range of applied stresses using Eq. (7). Note that when $\sigma_a = \sigma_0$, we have the safe condition of 1% crack growth in 40 years. Figure 2 is a plot of a/a_0 versus time t for a range of applied stress values σ_a/σ_0 and a material with an n of 20. These curves show that crack growth is minimal over most of the crack's lifetime and that the growth rate increases rapidly as the crack depth approaches twice its original size. At $a/a_0 = 3$, the crack velocity is more than five orders of magnitude greater than its initial value and the crack failure is very near ($t \approx t_f$). Taking

Table 1. Crack growth parameter V_0/a_0 for various values of n.

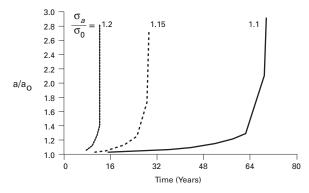|	n	$\dfrac{V_0/a_0}{(s^{-1})}$
	15	7.659×10^{-12}
	20	7.566×10^{-12}
	25	7.474×10^{-12}
	30	7.384×10^{-12}
	35	7.295×10^{-12}
	40	7.207×10^{-12}
	45	7.121×10^{-12}
Hermetic	200	5.017×10^{-12}

Fig. 2 Crack growth versus time under constant applied stress for n=20.

$a/a_0 = 3$ to be the crack length at failure, Eq. (7) becomes

$$t_f = \left(1 - 3^{-(n-2)/2}\right) \times \left(\frac{n}{2} - 1\right)^{-1} \left(\frac{V_0}{a_0}\right)^{-1} \left(\frac{\sigma_a}{\sigma_0}\right)^{-n} .$$

For $15<n<45$, we may neglect $3^{-(n-2)/2}$ compared to unity, and Eq. (8) simplifies to

$$t_f = \left(\frac{n}{2} - 1\right)^{-1} \left(\frac{V_0}{a_0}\right)^{-1} \left(\frac{\sigma_a}{\sigma_0}\right)^{-n} .$$

Equation (9) represents time to failure as a function of applied stress/safe stress ratio and is of the same form as that given by Eq. (1). Thus, the safe stress σ_0 for 1% crack growth in 40 yr can be determined from time to failure t_f versus applied stress σ_a data. We could stop here and perform short-term static fatigue experiments to determine σ_0; however, our goal is to provide a methodology that incorporates the fiber-strength distribution in addition to the fatigue parameter n. In Sec. 3.3 we will attempt to incorporate the measured-strength distribution into the safe stress model.

Before proceeding further, let us review two assumptions made up to this point: (1) the power law crack velocity equation is taken to represent subcritical crack growth in optical fibers; (2) we have selected the boundary condition of 1% allowable crack growth relative to the initial crack depth in 40 years. Condition (2) is meant to build safety into the power law fatigue model rather than rely on an arbitrary safety factor for the applied stress. In addition, it defines a threshold for static fatigue that has been observed in silicate glasses. The long-term experiment by Helfinstine provides some evidence for a threshold in fiber or, at the very least, extremely low crack velocities.

3.3 Incorporating fiber strength

In any reliability design for optical fiber, the flaw distribution over the fiber length must be incorporated into the reliability model. Equation (9) can be rearranged with the short-term static fatigue time to failure and applied stress together as

$$t_f \sigma_a^n = \left(\frac{n}{2} - 1\right)^{-1} \left(\frac{V_0}{a_0}\right)^{-1} \sigma_0^n .$$

The left-hand side of Eq. (10) gives short-term static fatigue data to predict long-term reliability on the right-hand side. Fiber strength is introduced into this model by equating the crack growth under static and dynamic loading conditions by

$$t_f \sigma_a^n = \sigma_f^{n+1} / \dot{\sigma}(n+1) \quad ,$$

where σ_f is the dynamic strength of the flaw that grows during testing at rate $\dot{\sigma}$, the same amount as it would under the static stress σ_a for time t_f. Equation (10) assumes that crack growth under both conditions obeys the same crack-growth curve, that is to say, the crack-growth parameters A and n from Eq. (3) are the same for both loading conditions. Recent research[9] has shown that n obtained in dynamic fatigue under saturated conditions is less than that obtained under static conditions for faster strain rates ranging from 4%/min to 0.004%/min. Below 0.004%/min, however, the dynamic n approaches the static n. These results indicate the possibility of a dependence of n and A on loading conditions. Additional research is currently in progress to compare predictions made from crack-growth parameters obtained under dynamic and static loading conditions.

Substituting Eq. (11) into Eq. (10) yields

$$\frac{\sigma_0}{\sigma_f} = \left[\frac{1}{2} \left(\frac{n-2}{n+1} \right) \frac{V_0}{a_0} \frac{\sigma_f}{\dot{\sigma}} \right]^{1/n}$$

Whereas Eq. (10) relates short-term static fatigue to the safe stress condition, Eq. (12) relates the safe static stress to the short-term strength of measured under dynamic fatigue conditions. Note that the combination of $\sigma_f/\dot{\sigma}$ in Eq. (12) is simply the time to failure under dynamic loading conditions. Given the fiber strength, rate of testing, and the parameter n, the safe stress σ_0 can be calculated. Figure 3 is a plot of σ_0/σ_f versus n for high- and low-strength flaws using Eq. (12) with V_0/a_0 determined for 40-year life. Observe in Fig. 3 that the safe stress to strength ratio has a rather weak dependence on flaw size. Thus, for silica-clad fibers with a dynamic n of 20, the safe static stress is 1/3 the short-term strength. For titania-doped silica-clad fibers with dynamic n of approximately 30, the safe static stress is nearly half the short-term strength. For hermetic fiber with an n of 200, the ratio σ_0/σ_f, is shown to be 0.9; i.e., fiber with an n of 200 can be loaded to 90% of its short-term strength in a corrosive environment for 40 years.

There are several important observations that must be made at this point in the model. First, the use of Eq. (12) assumes that long-term su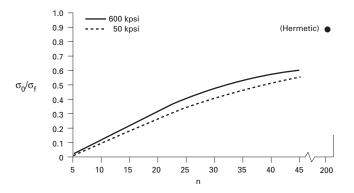bcritical crack-growth phenomenon is the same as that during short-term strength testing at rate $\dot{\sigma}$ and during fatigue testing at various rates to determine n. In addition, it is desirable that the strength term σ_f in Eq. (12) can be obtained from data tested in the same environment as that used to obtain n.

3.4 Incorporating the fiber-strength distribution

Fiber strength is not a material property, but rather a statistical parameter reflecting the distribution of flaw sizes on the glass surface. Thus, it is imperative that the fiber-strength distribution relevant to the application be incorporated into the design for mechanical reliability.

Figure 4 shows an example of a 20-m gauge length strength distribution of 17 km of standard silica-clad fiber tested under ambient conditions at 4%/min strain rate. The distribution is not unimodal and generally can be described by three regions. The high strength of "intrinsic" region extends to the 5% failure probability level and a strength of approximately 500 kpsi (3450 MPa). A second region extends from the "knee" at 5% to another, more gradual, knee near a failure probability of 0.2%. The truncation of the distribution due to proof testing at 50 kpsi (350 MPa) is represented by the dashed line since no failures were observed below 75 kpsi (520 MPa). This final region is imposed on the strength distribution by proof testing, whereas the first two regions reflect the distribution of flaws induced by manufacturing and handling prior to proofing.

3.4.1 Short-length applications

A short-length application is one where only a few meters of fiber are placed under stress. Thus, we need measure only the high-strength region of the distribution. The high-strength region of the fiber distribution often can be described by a two-parameter Weibull distribution,[10]

$$\ln \ln \frac{1}{1-F} = m \ln S - m \ln \sigma'$$

where F is the failure probability, S is the short-term strength, and m and σ' are the Weibull modulus and scaling parameters, respectively. In the more classical time-to-failure methodology given in Eq. (1), the inert strength $S = S_i$ is expressed in terms of failure probability m and σ' using Eq. (13).[10] Thus, we can obtain the probability of failure for a given lifetime and applied stress. This

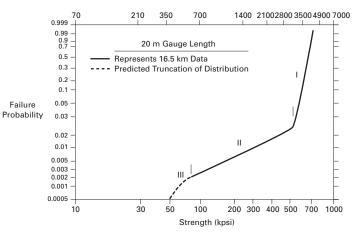Fig. 3 Ratio of safe stress to short-term strength as a function of n.

Fig. 4 Strength distribution of standard silica-clad fiber under ambient conditions.

technique is appropriate for very short length applications since inert-strength measurements are possible, and fiber-strength distributions usually can be described by the two-parameter Weibull distribution given in Eq. (13).

For the reliability model in this paper, the strength distribution is one measured under fatigue conditions $S=\sigma_f$, and the Weibull parameters in Eq. (13) are determined from a regression of $\ln\sigma_f$ versus $\ln \ln[1(1-F)]$. Solving for $S=\sigma_f$ in Eq. (13),

$$\sigma_f = \exp\left[\frac{1}{m}\ln\ln\frac{1}{1-F} + \ln\sigma'\right]$$

Substituting Eq. (14) into the model in Eq. (12) yields

$$\sigma_0 = \exp\left[\frac{1}{m}\ln\ln\frac{1}{1-F} + \ln\sigma'\right] \times \left[\frac{1}{2}\left(\frac{n-2}{n+1}\right)\frac{V_0}{a_0}\frac{\bar{\sigma}_f}{\dot{\sigma}}\right]^{1/n},$$

where a median strength $\bar{\sigma}_f$ suffices for obtaining an approximate time to failure under dynamic loading $t_d = \bar{\sigma}_f / \dot{\sigma}$. Thus, for a measured-strength distribution and n value, we can estimate the required safe stresss for a desired failure probability.

In the classical design methodology, failure probability means the time for catastrophic failure. In our present context, however, failure probability means the probability of exceeding 1% crack growth over the next 40 yr. For example, installed silica fiber splices are loaded to 20 kpsi (140 MPa) for the next 40 yr and have a failure probability requirement of 1 failure per every 1000 splices. From our model the $\sigma_0/\sigma_f = 1/3$ for silica fiber ($n=20$) or $\sigma_f = 20\times3 = 60$ kpsi (410 MPa). Failure, in this case, means having more than one flaw at or below 60 kpsi (410 MPa) per 1000 splices.

3.4.2 Long-length applications

Applications that use long fiber lengths can be single systems employing kilometers of fiber like the submarine application or multiple smaller systems such as coupler pigtails that eventually add up to long lengths when many of them are installed. It is essential in these cases that the design for reliability include the strength distribution of many *kilometers* of fiber.
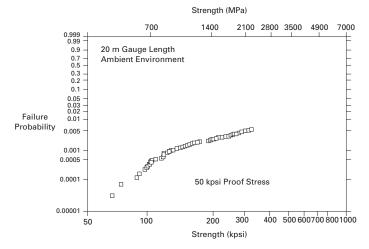

Fig. 5 Strength distribution of 386 km of titania-doped silica-clad fiber.

To incorporate the long-length strength distribution into Eq. (12), focus is placed on the lower regions of the strength distribution shown in Fig. 4, since the high-strength region is of a lesser interest in long-length applications. To make failure probability predictions near the proof stress level, it has been necessary for engineers to extrapolate through the truncated portion of the strength distribution from data in region II.[11] This extrapolation requires knowledge of the proof test environment, fatigue behavior of the fiber, and the proof test dwell time and unloading rate. The statistical theory for such extrapolations has been well documented[12]; however, extrapolations still must be made over many orders of magnitude in failure probability.

Recently researchers at Corning have developed a technique for strength testing long lengths of fiber in tension in a relatively short period of time.[13] Figure 5 shows strength data below 350 kpsi (2410 MPa) from 386 km of fiber tested in tension using 20-m gauge lengths. To test such long fiber lengths, the low-risk high-strength flaws that, from Fig. 4, normally occupy 95% of the test time are ignored by the test equipment. The distribution in Fig. 5 shows the beginning of the truncated region of the strength distribution. With this technique, it is possible to measure the distribution of flaws near the proof stress level for several thousand kilometers of fiber in a relatively short period of time. Such data would greatly reduce the extrapolated distance over which failure probability predictions are made. For example, a 5000-km strength distribution would yield data down to failure probabilities of 1×10^{-4}/km.

3.4.3 Minimum-strength design

In the absence of a long-length strength distribution, engineers have, in the past, chosen to design around the minimum strength.[3,10] For the present model under consideration, the minimum strength is that obtained under fatigue conditions *after* the fiber has been proof tested. The minimum *fatigue* strength $\sigma_f = \sigma_{fmin}$, after proof testing in our safe stress model, given by Eq. (12), is significantly less than the proof stress due to crack growth during the postproof strength test under fatigue conditions. Experimental evidence for fatigue susceptible soda-lime-silica glass suggests that flaws in bulk glass degrade approximately 30% in strength during strength testing in a fatigue environment.[14] Thus, for flaws that just pass the proof test, a 30% degradation in strength from the proof stress is taken to be the minimum postproof strength in a fatigue environment of $\sigma_{fmin} \approx 0.7\ \sigma_p$ for both silica- and titania-doped silica-clad fibers. Note that this estimate of the minimum strength assumes strength degradation during the unloading portion of the proof test to be small due to the extremely fast unloading rates of present-day high-speed screeners.[10] In addition, this analysis does not account for strength degradation due to incidental fiber damage after proof testing, and thus, it is preferable to measure the strength distribution rather than predict it.

Substituting $\sigma_f = \sigma_{fmin} = 0.7\ \sigma_p$ into the model in Eq. (12) for silica- and titania-doped silica-clad fibers, a design rule for long-length applications is obtained where the allowable safe static stress is expressed as a fraction of the proof stress:

$$\frac{\sigma_0}{\sigma_p} = 0.7\left[0.35\left(\frac{n-2}{n+1}\right)\frac{V_0}{a_0}\frac{\sigma_p}{\dot{\sigma}}\right]^{1/n} \quad \text{for silica- and titania-doped silica-clad.}$$

Equation (16) is plotted in Fig. 6 for the same conditions previously given for Fig. 3. From Fig. 6 the predicted safe stress for silica-
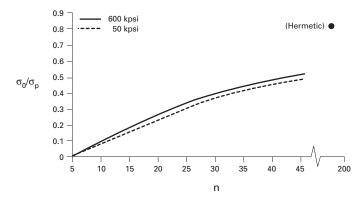
Fig. 6 Ratio of safe stress to proof stress as a function of n.

Table 2. Allowable stress design rules.

Fiber type	n dynamic	installation 24 Hours	long-term 40 years
Based on Fatigue Strength, σ_0/σ_f			
Silica-clad	20	0.5	0.3
Titania-doped silica-clad	30	0.6	0.5
Hermetic	200	0.9	0.9
Based on Fatigue Strength, σ_0/σ_p ($\sigma_{fmin} = 0.7\sigma_p$ in Eq. (12))			
Silica-clad	20	0.35	0.20
Titania-doped silica-clad	30	0.42	0.35
Hermetic	200	0.80	0.80

clad fiber is approximately 1/5 the proof stress, whereas it is 1/3 for the titania-doped silica-clad fiber. In the case of hermetic fiber, the post-proof-test minimum strength obtained in a fatigue environment σ_{fmin} is very nearly equal to the proof stress σ_p since virtually no crack growth occurs during the strength test. To be conservative, a minimum strength design rule of $\sigma_0=0.80\sigma_p$ is recommended.

It is acknowledged that little data exist on fiber to verify the use of 70% strength degradation from the proof-stress level during postproof strength testing and that further testing is needed. However, rather than use a percentage of the proof stress as the minimum strength, as discussed above, the authors stress the need for long-length strength distributions, wherefrom we model in terms of failure probability even for very long-length applications.

4. SAFE INSTALLATION STRESSES

In addition to 40-yr reliability, the possibility of crack growth during installation requires tha we predict safe installation stresses. For long life, we chose a safe condition of 1% crack growth over 40 years. For installation, we chose a safe condition of 1% crack growth in 24 h. Following the same analysis for long-life similar design, rules are developed for installation and are shown in Table 2 along with the previously determined long-life design rules. Note that the hermetic rules for both installation and long-term reliability are the same and reflect a conservative engineering estimate even though it is not expected to fatigue.

5. SUMMARY

Conventional fracture mechanics and fatigue theories were used to build a framework for estimating a safe stress value for the long-term mechanical reliability of optical fibers. At the center of the analysis is the concept of a threshold or safe stress for fatigue in glass, which is based on a boundary condition of 1% crack growth in 40 yr. A design rule for mechanical reliability was derived in terms of applied stress as a fraction of short-term fatigue strength for a range of n values. Knowing that fiber strength is a statistical parameter, a technique for measuring the strength distribution of kilometers of fiber was developed in order to minimize the distance over which failure probability predictions are made. Thus, this methodology enables us to make long-term failure probability predictions provided the fiber n value and strength distribution are appropriate for the application. Finally, the methodology was extended to safe allowable installation stresses and, in an empirical fashion, to minimum strength designs where the safe allowable stress was expressed as a fraction of the fiber proof stress.

It is important to note that in most applications the applied stress varies over the fiber length. This can be accounted for by using well-established probabilistic models. We also may use the proposed design methodology for determining the overall mechanical reliability of a system or link, which is especially important for local-loop and undersea systems.

6. REFERENCES

1. T. A. Michalske and S. W. Freiman, "A molecular interpretation of stress corrosion in silica," *Nature*, 295(2), 511-512 (1982).
2. S. T. Gulati, "Crack kinetics during static and dynamic loading," *J. Non-Cryst. Solids* 38-39, 475-480 (1980).
3. A. G. Evans and S. M. Wiederhorn, "Proof testing of ceramic materials. An analytical basis for failure predictions," *Int. J. Frac.* 10, 379-392 (1974).
4. S. T. Gulati et al., "Improvements in optical fiber reliability via high fatigue resistant composition," in *Fiber Optics Reliability: Benign and Adverse Environments*, Proc. SPIE 842, 22-31 (1987).
5. S. M. Weiderhorn, "Influence of water vapor on crack propagation in soda-lime glass," *J. Am. Ceram. Soc.* 50(8) 407-414 (1967).
6. B. R. Lawn and T. R. Wilshaw, *Fracture of Brittle Materials*, Cambridge University Press, London (1975).
7. K. Jakus et al., "Dependency of fatigue predictions on the form of the crack velocity equation," *J. Am. Ceram. Soc* 64(6), 372-374 (1981).
8. R. J. Charles, "Static fatigue of glass: I, II," *J. Appl. Phys.* 29(11), 1657-1662 (1958).
9. G. S. Glaesemann and S. T. Gulati, "Dynamic fatigue data for fatigue resistant fiber in tension vs. bending," in *1989 Technical Digest Series, Vol. 5*, Proc. Optical Fiber Communication Conference, 48 (1989).
10. J. E. Ritter, Jr., "Assessment of reliability of ceramic materials," in *Fracture Mechanics of Ceramics, Vol. 5*, R. C. Bradt, A. E. Evans, D. P. H. Hasselman and F. F. Lange, eds., pp. 227-251, Plenum, New York (1983).
11. Y. Mitsunaga, Y. Katsuyama, H. Kobayashi and Y. Ishida, "Failure prediction for long length optical fiber based on proof testing," *J. Appl. Phys.* 53(7), 4847-4853 (1982).
12. J. E. Ritter, Jr., P. B. Oates, E. R. Fuller, Jr. and S. M. Wiederhorn, "Proof testing of ceramics, part 1: experiment," *J. Mater. Sci.* 15, 2275-2281 (1980); see also E. R. Fuller, Jr., S. M. Wiederhorn, J. E. Ritter, Jr., and P. B. Oates, "Proof testing of ceramics, part 2: theory," *J. Mater. Sci.* 15, 2282-2295 (1980).
13. G. S. Glaesemann and D. J. Walter, "Method for obtaining long-length strength distributions for reliability predictions," *Opt. Eng.* 30(6) (1991).
14. J. E. Ritter, Jr., G. S. Glaesemann, K. Jakus, and P. Rampone, "Dynamic fatigue of soda-lime glass as a function of temperature," *Phys. and Chem. of Glasses* 27(2), 65-70 (1986).

G. Scott Glaesemann is a senior development engineer responsible for the optical waveguide strength laboratory at Corning. He has been employed by Corning for five years at the Sullivan Park research and development facility. Glaesemann received his master's degree and Ph.D. in mechanical engineering from the University of Massachusetts and a BS in mechanical engineering from North Dakota State University. He is a member of the American Ceramic Society.

Suresh Gulati is a research fellow responsible for the long-term reliability of Corning's products, including optical fiber, ceramic substrates, and fused-silica windows. Gulati joined Corning in 1967 as a senior research scientist in mathematics and mechanics. In 1974, he became a research associate in physical properties, advancing to senior research associate in 1979. Gulati was named a Corning research fellow in 1983. His research interests include the behavior of brittle materials subjected to mechanical and thermal loads, design of glass and ceramic products, strengthening methods for glasses, and fatigue and fracture of brittle materials. Before joining Corning, Gulati held positions with Cornell University, the University of Colorado, and Continental Can Company. Gulati holds a Ph.D. in mechanics from the University of Colorado, Boulder, an MS in mechanical engineering from Illinois Institute of Technology in Chicago, and a BS in mechanical engineering from University of Bombay, India. He is a member of the American Ceramic Society and the American Society of Mechanical Engineers.